meeting of the American Society of Civil Engineers and the Engineering Institute of Canada, John Clark of Alcoa concluded: "In the main, it has been shown that aluminum in bridges give trouble-free, maintenance-free service--up to 28 years in the examples cited."

Ten years later, the 1983 survey of these same bridges leads to a similar conclusion. On the basis of engineering applicability, aluminum is now a proven material for bridge construction. Any initial cost premium is more than justified by low maintenance and long life.

Publication of this paper sponsored by Committee on General Structures.

Finite-Element Load Distribution Factors for Multi-T-Beam Bridges

PATRICK R. REISNOUR and FAHIM A. BATLA

ABSTRACT

In this paper the determination of the lateral distribution of wheel loads on multi-T-beam bridges using the finite-element method is presented. The results are compared with existing applicable AASHTO specifications and other methods found in the literature. The evaluation of lateral wheel load distribution is of importance because of the significance of the localized effects of wheel loads on stresses and deflections of individual T-beams and must be determined with sufficient accuracy. It is found that significant differences exist in wheel load distributions determined using applicable specifications and other methods compared with distributions determined using the finite-element method of structural analysis.

The use of precast concrete components for the construction of multi-T-beam bridge superstructures with short to medium span lengths is increasing because of the ease of construction and relative economy associated with this type of superstructure. Because of the complexity of the behavior of multi-T-beam superstructures, the bridge engineer must often rely on design aids to avoid the complicated mathematical procedures of a rigorous analysis. These design aids should be simple to use yet lead to sufficiently accurate designs.

For bridges with short to medium spans, considerable emphasis must be placed on the calculation of stresses and deflections due to wheel loads. This emphasis is necessary because the local effects of these loads are of considerable significance in comparison with those effects caused by the other loads on the superstructure that are better distributed both longitudinally and transversely. Therefore the lateral distribution of wheel loads on multi-T-beam superstructures must by determined with a considerable degree of accuracy.

In this paper a comparison of factors used for the lateral distribution of wheel loads on nonskewed multi-T-beam superstructures obtained by several methods is presented. The load distribution factors that are based on existing design aids and other methods are compared with distribution factors determined using modern techniques of structural analysis based on the finite-element method. In the finite-element method, T-beam-type or similar structural systems are represented as an assemblage of plate finite elements and the overall behavior of the structure is then represented by the interaction of in-plane and out-of-plane plate deformations of the plate elements.

A multi-T-beam bridge superstructure is constructed by placing single-, double-, or multiple-stem T-beams side by side on the supports (Figure 1). In this investigation the flanges of adjacent T-beams are assumed to be connected throughout the length of the superstructure in a manner that provides full transfer of transverse shear and bending moments between the beams. The behavior of a multi-T-beam superstructure can be represented as the interaction of the longitudinal bending, transverse bending, and torsional behaviors of the superstructure (Figure 2). These individual aspects of the overall behavior of the structure are in turn dependent on structural parameters such as span lengths and thickness of the flanges and stems. The distance between the stems, width of the superstructure, depth of the stems, and position of wheel loads also affect the behavior of the superstructure. The parameters, which influence the distribution of wheel loads, that are varied in this study include

1. Span length,
2. Width of the superstructure,
3. Depth of the superstructure,

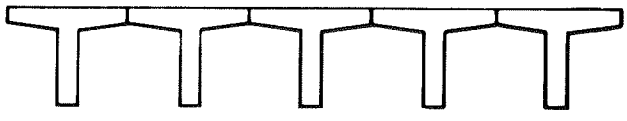

FIGURE 1 Cross section of multi-T-beam superstructure.

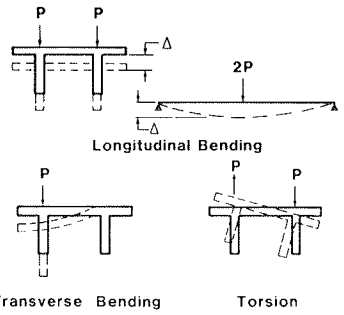

FIGURE 2 Deflection behavior.

4. Transverse position of the wheel loads,
5. Longitudinal position of the wheel loads, and
6. Number of traffic lanes.

The following parameters influence the lateral distribution of wheel loads and are the same for all the superstructures analyzed in this study.

1. Spacing of beams,
2. Flange thickness,
3. Thickness of stems,
4. Location of diaphragms, and
5. Span-to-depth ratio.

It should be noted that, in the course of developing final design aids for determining wheel load distribution factors for multi-T-beam superstructures, the influence of the parameters that may affect the lateral distribution of wheel loads must be thoroughly investigated. This is a monumental task. However, this task can be made easier and the results more accurate by use of the finite-element method of structural analysis.

To initiate the comparison of wheel load distribution factors based on various methods of analysis, it is useful to first discuss the theories on which the analysis methods and design aids are based. The discussion of theories and methods of analysis is presented in the next section. This is followed by the presentation and discussion of the results of the investigation described previously.

METHODS OF ANALYSIS

The finite-element method, the provisions of Article 1.3.1(B) of AASHTO Standard Specifications for Highway Bridges (1), and procedures developed by Aziz et al. (2) are used to determine distribution factors for wheel loads in this study. The finite-element method is used to determine the distribution of stresses and deflections in multi-T-beam superstructures and single T-beams. These distributions are in turn used to calculate the distribution factors. Distribution factors are determined using AASHTO design aids based on the spacing between the stems (1) and, in the procedures presented by Aziz (2), the calculation of distribution factors requires the evaluation of several dimensionless stiffness coefficients of the superstructure.

The AASHTO provisions for load distribution on beam and slab bridges, which are revisions to the specifications proposed by Sanders and Elleby (3), and the procedure presented by Aziz et al. (2) are based on analyses of bridge superstructures using orthotropic plate theory and tests conducted on actual bridges.

In orthotropic plate theory, the behavior of the superstructures is modeled as the behavior of a plate with uniform thickness and uniform but different flexural properties in the transverse and longitudinal directions (4-6). The actual flexural properties in the transverse direction of a multi-T-beam superstructure are not uniform across the width because of the localized contribution of the torsional stiffness of the stems to the transverse bending stiffness of the flange. However, in orthotropic plate theory, the transverse bending stiffness of the orthotropic plate is taken as the uniform distribution of the actual flexural stiffness.

In addition to the assumption of uniform flexural properties in the transverse and longitudinal directions, assumptions pertaining to classical thin plate theory are also used in the orthotropic plate approach (4-6). Furthermore, the following assumptions are used by Sanders and Elleby (3).

1. Poisson's ratio is equal to zero,
2. All connections transfer full moment and shear,
3. The spacing between beams and diaphragms is uniform,
4. The superstructure is rectangular in plan,
5. The beams are of equal stiffness, and
6. The superstructure behaves elastically.

With the exception of the first of these assumptions, the same assumptions were used for the analyses of multi-T-beam superstructures by Aziz et al. (2). Furthermore, in the analyses it is assumed that no intermediate diaphragms are used in the superstructure (2).

Application of the orthotropic plate model to represent the behavior of a multi-T-beam superstructure consists of representing the superstructure as a flat plate simply supported at the ends and free along the longitudinal edges. In superstructures where the spacing between stems or the depth of the stems is large in comparison with other dimensions of the T-beams, the orthotropic plate model presents a gross simplification of the actual behavior of the superstructure because of the manner in which the transverse and longitudinal bending stiffnesses and the torsional stiffness are treated.

In superstructures with large spacings between the stems, or deep stems, or both, the localized transverse stiffness of the flange in the vicinity of the stems creates a condition of transverse bending similar to the bending of a beam that is continuous over elastic supports (Figure 3). These elastic supports (stems) provide resistance to rotation (due to torsional stiffness of the stem) and resistance to vertical translation (due to longitudinal bending stiffness of the superstructure). Therefore, to arrive at a sufficiently accurate solution for the behavior under load of a multi-T-beam superstructure, the use of orthotropic plate theory is limited to those superstructures where the dimensions of the individual T-beams are such that the uniform transverse bending stiffness of the orthotropic plate

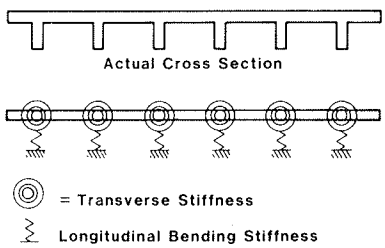

FIGURE 3 Continuous beam analogy.

does not differ greatly from the actual stiffness at any transverse location in the flange.

As noted previously, the lateral distribution of wheel loads is affected by the longitudinal and transverse bending behavior and the torsional behavior of the superstructure. The longitudinal bending behavior of the superstructure produces longitudinal in-plane stresses in the flange and stems (Figure 4). The transverse bending moments produce transverse distortions of the stems and flanges in the plane of the cross section that in turn influence the torsional properties of the cross section.

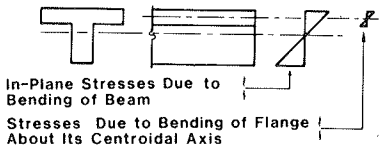

FIGURE 4 Longitudinal stresses caused by bending.

In Figure 4 it can be seen that the thickness of the flanges is small in comparison with the overall depth of the structure. The longitudinal in-plane stresses in the flange due to longitudinal bending of the flange plates about their centroidal axes are quite small in comparison with the longitudinal in-plane stresses in the flange due to the longitudinal bending of the T-beam cross section about its neutral axis. Hence, the longitudinal plate bending stresses of the flange due to bending about its centroidal axis can be neglected. Furthermore, because the longitudinal dimensions of the flange are much greater than the transverse dimensions between the stems, the bending of the flange may be treated as predominantly one-way (transverse) bending. Similar reasoning can be applied to the stems to show that they are also subject to one-way bending in the direction across the depth of the stem. Multi-T-beam superstructures can therefore be classified as folded plate structures that consist of long flat plates joined at the folds.

The finite-element method of structural analysis provides a means of accurately representing the actual geometry of multi-T-beam superstructures as well as the actual loading and support conditions. Furthermore, the finite-element method eliminates the need to make several simplifying assumptions typically used in the analysis of folded plate structures with other analytic techniques and formulations (7,8). Modeling of a multi-T-beam superstructure using the finite-element method eliminates the need to assume that the transverse bending stiffness is a uniform distribution of the actual stiffness because the actual distribution of the transverse bending stiffness is represented by the model. Finite-element modeling also provides an accurate representation of the longitudinal and twisting behavior of the structure. The finite-element method of structural analysis in general uses the assumptions of classical thin plate bending and in-plane elasticity theories because model developments are typically based on these theories. If these assumptions are satisfactory, the finite-element method leads to a much more accurate and straightforward analysis than do simplified methods of analysis. The accuracy of the finite-element models used in this study is demonstrated elsewhere (9-11) where results of finite-element analyses are compared with experimental results and results based on elasticity solutions that are considered exact.

Two finite-element programs are used for the analysis of multi-T-beam superstructures in this study. The finite-element program FAP, which was developed by Batla (11) specifically for the elastic analysis of constant-depth, straight folded, plate structures, is used as is the finite-element program SAPIV (12). The FAP program is used to determine the distribution of stresses and deflections due to wheel loads (two wheel loads per traffic lane) in all the multi-T-beam superstructures considered in this study. The SAPIV program is used as a finite-element analysis to provide independent verification of the results. The stresses and deflections, due to one wheel load on the beam, are also determined in a single T-beam. The longitudinal location of the wheel loads is the same for the superstructure and the single T-beam. The transverse locations of the wheel loads on the superstructures are discussed in the next section. The load factor representing the lateral distribution of wheel loads is determined as the ratio of the maximum stress in the superstructure to the maximum stress in the single T-beam. Load factors are determined from comparison of maximum peak stresses that occur in the flange above the stems, comparison of the maximum tensile stresses that occur at the bottom of the stems, and comparison of the maximum deflections that occur in the superstructure and single T-beams. The load factors determined using the finite-element analysis and those determined using the methods discussed previously are presented in the next section. The load factors based on comparison of the compressive stresses, tensile stresses, and deflections using the SAPIV finite-element program (12) are also presented to compare the load factors determined using different finite-element models.

DETERMINATION OF WHEEL LOAD DISTRIBUTION

The multi-T-beam superstructures for which wheel load distributions are determined in this study are assumed to be constructed of single-stem T-beams. The span-to-depth ratio, spacing between stems, flange thickness, and stem width are the same for each superstructure (Figure 5). The superstructures considered here consist of two overall widths: two-lane superstructures constructed of five T-beams, and superstructures constructed of seven T-beams. The latter are analyzed as both two-lane and three-lane bridges (Figure 6).

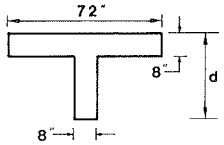

Span Length Feet	d Inches
40	24
60	36
80	48
100	60

FIGURE 5 Cross section of typical single T-beam.

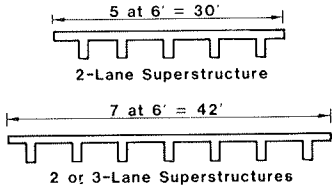

FIGURE 6 Superstructure cross sections.

In the finite-element method, the superstructures and single T-beams are modeled as simply supported with end diaphragms that are infinitely rigid in their own plane but completely flexible in the direction normal to the plane of the diaphragms; no intermediate diaphragms are used. The wheel loads on the superstructure are applied at midspan as well as at a distance from the midspan that represents the location of the wheels of an AASHTO HS 20-44 truck load with the center of gravity of the truck near the midspan (Figure 7). The lateral location of wheel loads considered for the evaluation of load factors is such that the loads act in the plane of the stems (Figure 8).

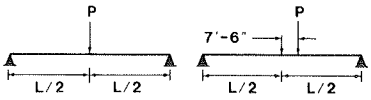

FIGURE 7 Longitudinal location of wheel loads.

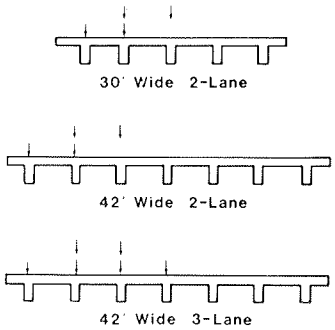

FIGURE 8 Transverse location of wheel loads.

As shown in Figure 8, two wheel loads are applied on stems that are common to two lanes. For convenience the finite-element idealization of the structure is done so that concentrated loads can be applied at the nodes. The wheel load cases shown in Figure 8 represent cases in which trucks are side by side and their wheel loads are close enough together to be assumed to be acting at the same point. The wheel loads are applied directly above the stems to ensure that the maximum compressive and tensile stresses occur at the top and bottom of the stems, respectively.

The maximum stresses and deflections in the multi-T-beam superstructures shown in Figure 6 and corresponding single T-beams are presented by Reisnour in his study of the lateral distribution of wheel loads on multi-T-beam bridges (10). The distribution of compressive stresses, due to single wheel loads placed at midspan, in the flange of a two-lane, 40-ft-span superstructure is shown in Figures 9 through 11. Figure 9 shows the stresses due to a wheel load over the stem of the central T-beam. The stress distributions shown in Figures 10 and 11 are due to single wheel loads placed on the T-beam adjacent to the central beam and the rightmost T-beam, respectively. Figures 12 and 13 show the distribution of compressive stresses in the flange due to two wheel loads in two positions at midspan. To illustrate the difference in the distribution of stress and deflections, the distribution of deflections due to the similar loading conditions for the same superstructures is presented in

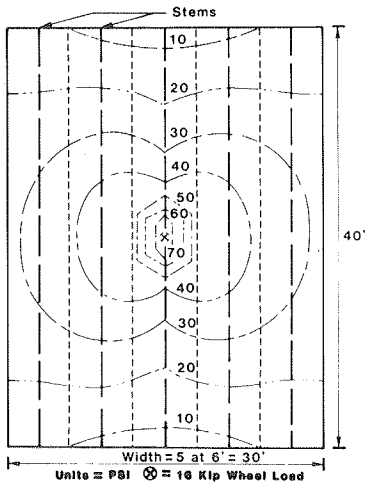

FIGURE 9 Compressive stresses in flange caused by single wheel load over stem of central T-beam.

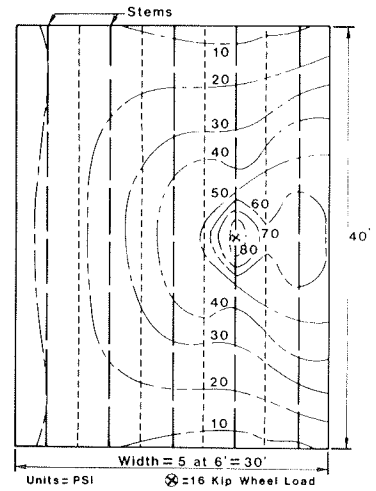

FIGURE 10 Compressive stresses in flange caused by single wheel load on T-beam adjacent to central stem.

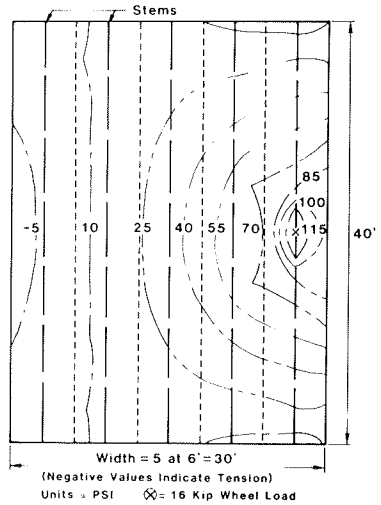

FIGURE 11 Compressive stresses in flange caused by single wheel load on rightmost T-beam.

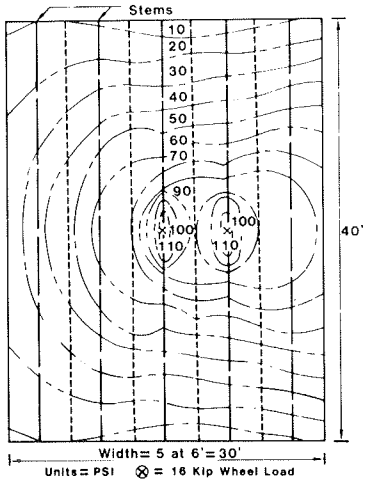

FIGURE 12 Compressive stresses in flange caused by two wheel loads: position 1.

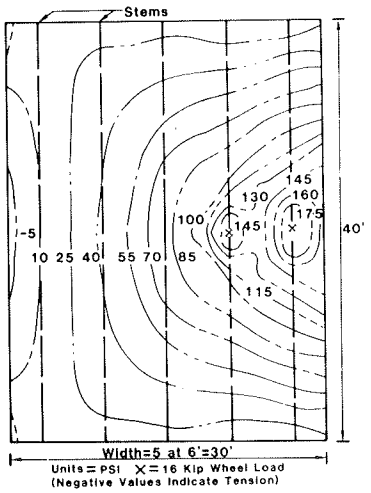

FIGURE 13 Compressive stresses in flange caused by two wheel loads: position 2.

Figures 14 through 18. The deflections shown in Figures 14 through 16 are those due to single wheel loads, and Figures 17 and 18 show the deflections due to two wheel loads.

The wheel load distribution factors based on maximum peak compressive stresses in the flange, maximum tensile stresses at the bottom of the stems, and maximum deflections as determined using the finite-element program FAP for the analysis of the superstructures shown in Figure 6 are presented in Table 1. Also given in Table 1 are the load factors calculated using the SAPIV finite-element program (12) for the 30-ft-wide, 40-ft-span superstructure to indicate the reliability of load factors determined using the different finite-element models. These distribution factors are calculated using the stresses and deflection due to wheel loads placed at the midspan of the superstructures and single T-beams. Distribution factors calculated using the stresses and deflections due to wheel loads placed at a distance from the midspan are not presented because they are similar to those shown in Table 1.

According to AASHTO provisions [1, Article

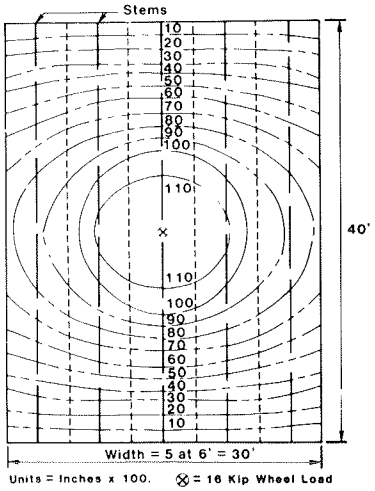

FIGURE 14 Deflections caused by single wheel load: position 1.

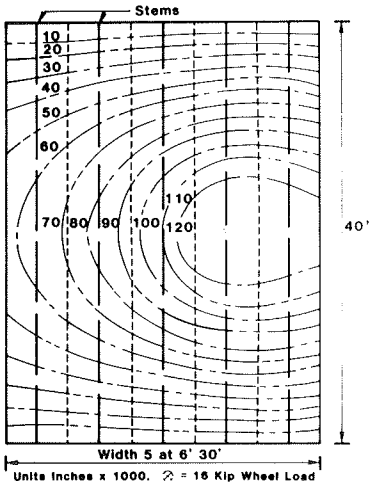

FIGURE 15 Deflections caused by single wheel load: position 2.

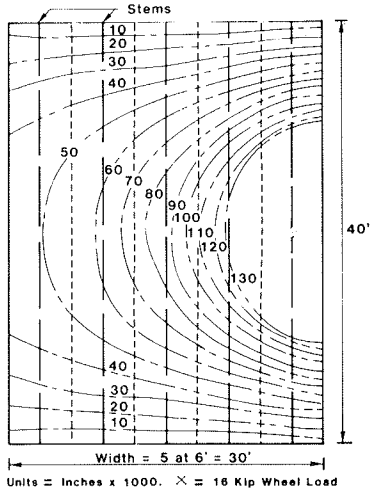

FIGURE 16 Deflections caused by single wheel load: position 3.

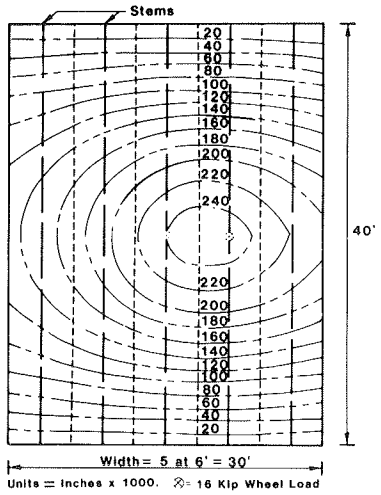

FIGURE 17 Deflections caused by two wheel loads: position 1.

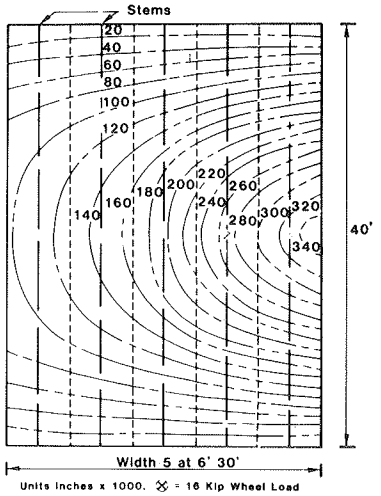

FIGURE 18 Deflections caused by two wheel loads: position 2.

TABLE 1 Load Distribution Factors Based on Compressive Stresses, Tensile Stresses, and Deflections as Determined Through Finite-Element Analyses

Span (ft)	Width (ft)	No. of Lanes	Based on Compressive Stresses	Based on Tensile Stresses	Based on Deflections
40	30	2	1.23	1.14	1.04
	30	2	1.29[a]	1.10[a]	1.02[a]
	42	2	1.19	1.06	0.93
	42	3	1.47	1.34	1.19
60	30	2	1.25	1.16	1.11
	42	2	1.17	1.07	0.96
	42	3	1.46	1.35	1.19
80	30	2	1.28	1.15	1.10
	42	2	1.19	1.06	0.99
	42	3	1.45	1.34	1.22
100	30	2	1.30	1.14	1.11
	42	2	1.20	1.05	0.99
	42	3	1.47	1.33	1.24

[a]Based on analyses using SAPIV; all other results are based on use of FAP.

1.3.1(B)], the wheel load distribution factor for a beam and slab superstructure, with two or more traffic lanes, constructed of concrete T-beams is determined as

$$LF = S/6$$

where

S = spacing between stems (feet).

Because the spacing between stems of all the superstructures considered in this study is 6 ft, the distribution factors for these superstructures are all equal to 1.

The procedure for determining distribution factors for multi-T-beam superstructures using the design aids presented by Aziz et al. (2) involves calculation of two nondimensional coefficents that are functions of the stiffness parameters of the superstructure. These coefficients are used to determine the coefficient D from charts presented in their paper (2). This coefficient D is corrected using a parameter that is a function of the width of the traffic lanes. The distribution factor is then calculated as

$$LF = S/D'$$

where

S = spacing between stems (feet) and
D′ = corrected D (feet)

The maximum wheel load distribution factors for each superstructure calculated using the finite-element method presented in Table 1 are given in Table 2 along with the distribution factors determined using the design aids of AASHTO (1) and Aziz et al. (2).

TABLE 2 Load Distribution Factors Based on Various Methods

Span (ft)	Width (ft)	No. of Lanes	Method: Finite Element	Method: AASHTO (1)	Method: Aziz et al. (2)
40	30	2	1.23	1.00	1.11
	42	2	1.19	1.00	1.17
	42	3	1.47	1.00	1.15
60	30	2	1.25	1.00	1.09
	42	2	1.17	1.00	1.13
	42	3	1.46	1.00	1.07
80	30	2	1.28	1.00	1.08
	42	2	1.19	1.00	1.17
	42	3	1.45	1.00	1.11
100	30	2	1.30	1.00	1.07
	42	2	1.20	1.00	1.17
	42	3	1.47	1.00	1.09

SUMMARY AND DISCUSSION

The data presented in Table 1 indicate that wheel load distribution factors based on comparison of compressive stresses, tensile stresses, and deflections all differ for each of the given superstructures. Figures 9 through 13 and 14 through 18 illustrate the differences between the distribution of compressive stresses in the flange and deflections. The difference between distribution factors based on tensile stresses and those based on compressive stresses indicates that there is a difference in the manner in which these stresses are distributed. This difference in the distribution of compressive

and tensile stresses is due to the presence of shear lag at the junction of the flange and stems; there is no shear lag effect at the bottom of the stems. The stress distributions shown in Figures 9, 10, and 12 show the occurrence of shear lag where the space between consecutive contours decreases more sharply along the loaded stem of the T-beam than at other locations across the width.

Figure 11 shows a region in the flange where a longitudinal stress reversal occurs at one side of the superstructure when the wheel load is located near the other edge. In the orthotropic plate model the superstructure is treated as a flat plate simply supported on the ends, free along the edges, and with uniform properties in the transverse and longitudinal directions. For this reason, under general wheel loading conditions, the orthotropic plate model of the superstructure will not be capable of predicting this stress reversal in the longitudinal direction of the superstructure, which may cause tensile stresses in the flange. Although the longitudinal stresses in the flange will be compressive when the dead load and other wheel loads are placed on the superstructure of the bridge shown in Figure 11, there may be cases, especially in structures where the width-to-span ratio is high, where the tensile stresses in the flange of the superstructure are quite significant and the net stress due to the superposition of all the loads may result in a longitudinal tensile stress in the flange.

Comparison of the distribution factors determined using the provisions of Article 1.3.1(B) (1) with the distribution factors calculated using the results of finite-element analyses (10) and the procedure presented by Aziz et al. (2) (Table 2) indicates that the latter methods of determining the lateral distribution of wheel loads on multi-T-beam superstructures are substantially different. The distribution factors determined using the stress distributions obtained from finite-element analyses and the procedure presented by Aziz et al. (2) are expected to be slightly higher because in both situations the superstructures are assumed to have no intermediate diaphragms. In the study by Sanders and Elleby (3) the superstructures were assumed to have intermediate diaphragms. It is interesting to note, however, that for the structures considered in this study, the wheel load distribution factors determined using the distribution of compressive stresses in the flange are quite conservative in comparison with the load factors calculated using the provisions of the AASHTO specifications.

To arrive at sufficiently accurate results of analyses of multi-T-beam superstructures, the model used to represent the behavior of the superstructure under load must be selected with great care. The use of orthotropic plate theory for the analysis of multi-T-beam superstructures must be limited to those superstructures where the uniform distribution of transverse bending stiffness does not differ greatly from the actual transverse bending stiffness at any point in the flange. The finite-element method is not limited to any particular geometrical configuration, loading or support conditions, or structural and material parameters. This method may be used, in conjunction with experimental testing of actual bridges, as the basis of simplified design aids without encountering the limitations found in other methods of analysis.

No matter what method of analysis is used for developing design aids for determining lateral wheel load distribution factors for multi-T-beam superstructures, it is important to discuss and clearly indicate in the specifications the limitations of application of the design aids in determining the lateral distribution of wheel loads. This will prevent inadvertant gross overdesigns or underdesigns.

ACKNOWLEDGMENT

The authors wish to express their appreciation to the staff of the North Dakota State University (NDSU) Computer Center and the faculty of the Department of Civil Engineering at NDSU for their encouragement, timely assistance, and advice throughout this project. Sincere thanks are also extended to R. Rogness of the Department of Civil Engineering for his advice and assistance in the preparation of this paper.

REFERENCES

1. Standard Specifications for Highway Bridges. 12th ed. AASHTO, Washington, D.C., 1977.
2. T.S. Aziz, M.S. Cheung, and B. Bakht. Development of a Simplified Method of Lateral Load Distribution for Bridge Superstructures. In Transportation Research Record 665, TRB, National Research Council, Washington, D.C., 1978, pp. 37-44.
3. W.W. Sanders and H.A. Elleby. Distribution of Wheel Loads on Highway Bridges. NCHRP Report 83. TRB, National Research Council, Washington, D.C., 1970, 56 pp.
4. R. Szillard. Theory and Analysis of Plates. Prentice-Hall, Englewood Cliffs, N.J., 1974.
5. A.C. Ugural. Stresses in Plates and Shells. McGraw-Hill, New York, 1981.
6. S. Timoshenko and S. Woinowski-Krieger. Theory of Plates and Shells. 2nd ed. McGraw-Hill, New York, 1959.
7. J. Born. Folded Plate Structures, Their Theory and Analysis. Translated by C.V. Amerongen. Fredrick Ungar, New York, 1962.
8. J.S.B. Iffland. Folded Plate Structures. Journal of the Structural Division, ASCE, Vol. 105, No. NST1, Jan. 1979, pp. 111-123.
9. F.A. Batla, V.J. Meyers, and P.R. Reisnour. Simplified Finite Element Analysis of Prismatic Folded Plates. Proc., International Symposium on Spatial Roof Structures, Dortmund, Federal Republic of Germany, Sept. 10-14, 1984.
10. P.R. Reisnour. Study of Lateral Distribution of Wheel Loads for Multi-Tee Beam Bridges. M.S. thesis, North Dakota State University, Fargo, 1982.
11. F.A. Batla. Finite Element Analysis of Prestressed Concrete Box Girders. Ph.D. dissertation, Purdue University, West Lafayette, Ind., 1976.
12. K.J. Bathe, E.L. Wilson, and F.E. Peterson. SAPIV: A Structural Analysis Program for Static and Dynamic Response of Linear Systems. PB-221 967. National Technical Information Service, U.S. Department of Commerce, June 1973.

Publication of this paper sponsored by Committee on General Structures.